

# Cavitation inception on micro-particles : a self propelled particle-accelerator

Claus-Dieter Ohl<sup>1</sup>, Manish Arora<sup>1</sup>, and Knud Aage Mørch<sup>2</sup>

1)Dep. of Appl. Physics, Physics of Fluids, TU Twente, Postbus 217, 7500 AE Enschede, The Netherlands

2)Dep. of Physics, Technical Univ. of Denmark, DK-2800 Lyngby, Denmark

Email: [c.d.ohl@tn.utwente.nl](mailto:c.d.ohl@tn.utwente.nl)

## Introduction

In experiments probing the threshold of cavitation inception for a liquid it is well known that the measured tensile strength is much weaker than the theoretically expected one. This is commonly attributed to gaseous and solid impurities within the liquid acting as nuclei for cavitation bubbles and termed heterogeneous cavitation. One of the candidates are particles [1] which stabilize attached pockets of gas being activated at sufficient tensile stress [2]. There, it is suggested that the surface properties of the particles play a decisive role for the stabilizing mechanism preventing the dissolution of the gas pockets, for example in hydrophobic cracks in the particle surface [3-6], or detachment of hydration layers at local concave surface corrugations [7].

In this paper we focus on the dynamics of a rapidly expanding bubble from a spherical micro-particle. We present high-speed photographs showing the explosive growth and the, at first sight unexpected, process of detachment of the particle from the surface of the cavity. Thereby, the particle gains a high initial speed,  $\approx 10$  m/s for the cases investigated here. The dynamics of the particle-cavity system is modeled with a force balance model describing the acceleration and detachment with sufficient accuracy. Finally, the system is reviewed in a broader perspective. With strong acoustic transients being able to accelerate particles by a generic mechanism of self propulsion it might allow for a novel method of drug delivery into biological cells if particles coated with or consisting of a specific drug are irradiated in a bulk solution next to cells.

## Experimental set-up and results

The experimental set-up, depicted in Fig. 1, consists of the shock wave source, a polystyrol flask containing the particles, the imaging and illumination devices and digital delay lines. A single shock wave is generated by a focused piezoelectric source; it is a slightly modified commercial extracorporeal lithotripter Piezolith 3000 (Richard Wolf GmbH, Knittlingen, Germany). The diameter of the shock wave source is 300 mm and the focusing angle  $94^\circ$ .

The axis of the source is placed at an angle of  $45^\circ$  to the horizontal plane at the bottom of a stainless steel container with glass windows on three sides. The container and the flask are filled with deionized and degassed water ( $O_2$  concentration 3.3 mg/l) at room temperature. The pictures are taken with a sensitive slow scan CCD camera (Imager 3S with  $320 \times 256$  pixels at a binning mode of  $2 \times 2$  and  $9 \mu\text{m}$  pixel size, LaVision GmbH, Germany) equipped with a long distance microscope (K2, CF4 lens, Infinity, USA). The microscope operates from a working distance of 45 mm giving a maximum resolution of  $3.4 \mu\text{m}$  per binned pixel. The CCD camera

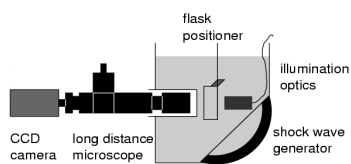


Figure 1: Experimental set-up.

is operated in a double-frame mode, which allows to take two images in rapid succession before they are transferred to a computer. Both frames are strobe illuminated with a LED (light emitting diode) driven by a home-built current amplifier for exposure times of  $1.8 \mu\text{s}$ . The light of the LED is coupled into a PMMA plastic fiber (1 mm core diameter) and brought to the illumination optics consisting of two lenses in order to collect and refocus the light while matching the numerical aperture of the long distance microscope. The illumination optics is sealed and submerged within the container. All devices are triggered from a digital delay generator (BNC 555, Berkeley Nucleonics Corp., USA); the two trigger pulses for the LED are generated with a programmable micro-controller.

The tensile stress wave has been measured with a fibre optical hydrophone to last for  $3.3 \mu\text{s}$ , and is followed by a next progressive stress wave. The flask contains filtered and degassed water seeded with globally spherical, hydrophilic polystyrol particles (Kopolymer: Styrol,2-Divinylbenzol, density  $\rho_p = 1.07 \text{ kg/m}^3$ ) with a diameter distribution between  $30 \mu\text{m}$  and  $150 \mu\text{m}$ .

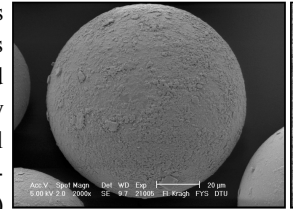


Figure 2: SEM image.

Figure 2 presents a scanning electron micrographs from an arbitrarily chosen subset of the particles from the same batch. A large group of these particles, though globally spherical, are characterized by a highly corrugated surface which possibly stabilizes gaseous cavitation nuclei. At discharge voltages above 5 kV corresponding to a peak tensile stress below  $-20$  MPa cavitation events were observed at some particles, but certainly not at all of them. For the high speed observations the camera was first operated in a continuous mode, displaying the motion of the particles due to gravity and secondary flow. When a particle is in the focal zone of the shock wave it is depicted sharply near the center of the imaged area, and now the camera is switched to a double frame-mode and the shock wave generator is activated. Thus, a first

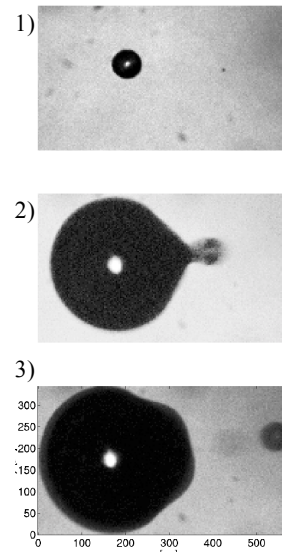


Figure 3: Cavity growth on a particle and its successive acceleration. Scale is in  $\mu\text{m}$ .

frame is taken approximately 500ms before the fast 2 frame sequence which have an inter-frame time adjustable in steps of  $1 \mu\text{s}$  duration. A resulting three frame sequence with the particle and an explosively expanding cavity being in focus is depicted in Fig. 3: The undisturbed particle,  $R_p = 34 \mu\text{m}$ , is depicted in frame 1. The shock wave with its tensile trailing wave impacts the particle  $8 \mu\text{s}$

before frame two where an attached cavity of radius 150 $\mu\text{m}$  has developed. The particle has been accelerated to the right, the cavity to the left. Frame three of Fig. 3 is taken 24.2  $\mu\text{s}$  after the impact of the shock wave. The cavity has expanded to an equivalent spherical radius of 170  $\mu\text{m}$ . The neck between the particle and the cavity eventually breaks, exciting the surface wave propagating on the cavity surface visible in frame 3.

### Force balance model

Let us consider a cavity that develops in water from a cavitation nucleus on the surface of an almost spherical particle of radius  $R_p$  when it is exposed to the tensile wave from the lithotripter; here we neglect the shock front. Such a wave is assumed to be described by

$$P_\infty = -P_a \sin(2\pi t/T_0) \exp(-t/\tau) \quad (1)$$

with  $P_a=4$  MPa,  $T_0= 6.6$   $\mu\text{s}$ , and  $\tau= 6.6 \cdot 10^{-6}$  s $^{-1}$ . For simplicity we assume that at the time  $t=t_{\text{crit}}$  when the tensile strength of the liquid-particle system is exceeded an attached spherical cavity of radius  $(R_c)_{\text{crit}}$  is developed, and that  $(dR_c/dt)_{\text{crit}} \approx 0$ . Further, it is assumed that the pressure changes sufficiently slow to ensure that the cavity experiences a uniform, quasistatic far field pressure distribution during its growth and collapse. Then the radial dynamics of the cavity is governed by the Rayleigh equation,

$$R_c \frac{d^2 R_c}{dt^2} + \frac{3}{2} \left( \frac{dR_c}{dt} \right)^2 = -\frac{P_\infty}{\rho_l} \quad (2)$$

where  $\rho_l$  is the liquid density, vapor pressure and surface tension are neglected. Now we focus on the translatory dynamics. In the time interval  $t_{\text{crit}} < t < t_{\text{sep}}$  no external forces influence the cavity-particle system, and thus momentum balance requires

$\int d/dt(mu) = 0$ , where  $m$  holds for the mass of the particle as well as for the added masses of the particle and the cavity. With the particle initially at rest the development of a single cavity from a small area of the particle surface implies that the expanding cavity and the particle move in opposite directions at increasing velocities  $u_c$  and  $u_p$ , respectively, see Fig. 3. The momentum balance Eq. (3) is valid until  $t=t_{\text{sep}}$ , for later times the added mass of the particle and the drag force has to be accounted for.

$$\frac{d}{dt} \left[ u_c \left( \frac{2}{3} \rho_l \pi R_c^3 \right) + u_p \left( \rho_p \frac{4}{3} \pi R_p^3 \right) \right] = 0 \quad (3)$$

The particle contact condition for times  $t < t_{\text{sep}}$  gives

$$\frac{d(x_c + R_c)}{dt} = \frac{d(x_p - R_p)}{dt} \quad (4)$$

or in terms of velocities

$$u_c + \frac{dR_c}{dt} = u_p \quad (5)$$

Integrating Eq. (3) and setting the constant zero, we can solve for the velocities  $u_p$  and  $u_c$  by applying Eq. (5):

$$u_p = \left( \frac{dR_c}{dt} \right) \left( 1 + \frac{2R_p^3 \rho_p}{R_c^3 \rho_l} \right)^{-1} \quad (6a)$$

$$u_c = - \left( \frac{dR_c}{dt} \right) \left( 1 + \frac{R_c^3 \rho_l}{2R_p^3 \rho_p} \right)^{-1} \quad (6b)$$

Figure 4 depicts the motion of the cavity (light gray) and that of the particle (dark gray) as a function of time. The initial cavity radius is 1  $\mu\text{m}$ , the tension wave, Eq. (1), starts at  $t=0$ . The solid lines depict the left end of the cavity and particle. They separate around  $t_{\text{sep}}=4.5$   $\mu\text{s}$ , the time of maximum deceleration of the cavity. The dashed lines in Fig. 4 denote the center of the cavity and the particle respectively. The cavity reaches a bubble radius of 160  $\mu\text{m}$  at time of separation,  $R_c(t=t_{\text{sep}})$ . The particle velocity at time of

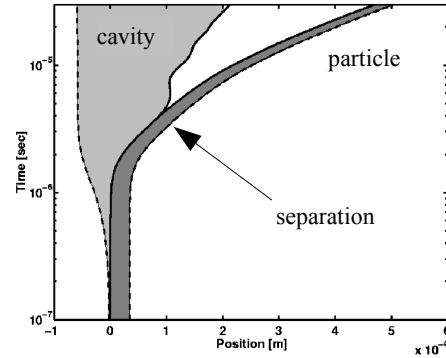


Figure 4: Position of cavity and particle after the tension wave is applied.

separation is equal to the cavity wall velocity of about 20 m/s which agrees reasonable well with the observed velocity of 10 m/s especially when taking into account the simplifying assumptions made.

### Conclusions

The novel findings suggest that most particles which are acting as a cavitation nuclei are propelled at considerable speeds away from the cavity when the tension is increasing back to atmospheric pressure. A possible beneficial application might be micro or nano-sized particles coated with specific drugs added to cell suspensions and activated through ultrasound. At chance, the self propelled particle penetrates the cell membrane and releases specific drugs or plasmids for transfection. In a more general view, the collapse of cavitation bubbles has received much of an attention whereas we show here, that some energy of the explosively expanding bubble is transferred to the particle during the inception. Possibly, these particle contribute to erosion of nearby surface at impact. The scenario of cavitation erosion by particle bombardment might be at later stages of cavitation erosion of higher importance when already some material removal has occurred and therefore, more nuclei for cavitation inception are supplied near the surface.

### Acknowledgments

We thank Detlef Lohse and Andrea Prosperetti for inspiring discussions. The research is granted by F.O.M. (The Netherlands) under 02PMT04 and 99MFS06.

### References

- [1] R.E. Apfel, Ultrasonics (1984) 167-173.
- [2] see for example, C.E. Brennen, *Cavitation and Bubble Dynamics*, Oxford Eng. Sci. **44** Oxford University Press 1995.
- [3] E.N. Harvey, D.K. Barnes, W.D. McElroy, A.H. Whiteley, D.C. Pease, K.W. Cooper, J. Cell Comp. Physiol. **24** (1944) 1-22.
- [4] M. Strassberg, J. Acoust. Soc. **31** (1959) 163.
- [5] R.E. Apfel, J. Acoust. Soc. **48** (1970) 1179.
- [6] Physics of Acoustic Cavitation in Liquids, in *Physical Acoustics*, Ed. W.P. Mason, Vol 1B, Academic Press, New York (1964) 57-172.
- [7] K.A. Mørch, J. Fluids. Eng. **122** (2000) 494.